J Appl Electrochem (2009) 39:1331–1337
DOI 10.1007/s10800-009-9800-y

ORIGINAL PAPER

Supercapacitive properties of composite electrodes consisting of polyaniline, carbon nanotube, and RuO_2

Jang Myoun Ko · Kwang Sun Ryu · Sanghyo Kim · Kwang Man Kim

Received: 9 September 2008 / Accepted: 16 January 2009 / Published online: 1 February 2009

Abstract Three types of composite supercapacitor electrodes were prepared; electroactive polyaniline (PANI), PANI/multi-walled carbon nanotube (CNT), and PANI/CNT/RuO_2. Specifically, the PANI and PANI/CNT were prepared by polymerization, and PANI/CNT/RuO_2 was prepared by electrochemical deposition of RuO_2 on the PANI/CNT matrix. Cyclic voltammetry between −0.2 and 0.8 V (vs. Ag/AgCl) at various scan rates was performed to investigate the supercapacitive properties in an electrolyte solution of 1.0 M H_2SO_4. The PANI/CNT/RuO_2 electrode showed the highest specific capacitance at all scan rates (e.g., 441 and 392 F g^{-1} at 100 and 1,000 mV s^{-1}, respectively). In contrast, the PANI/CNT electrode demonstrated the best capacitance retention (66%) after 10^4 cycles. Additional analysis including morphology and complex impedance spectroscopy suggested that with small loading of RuO_2, an increase in capacitance was observed, but dissolution and/or detachment of RuO_2 species from the electrode might occur during cycling to reduce the cycle performance.

Keywords Polyaniline · Carbon nanotube · Ruthenium oxide · Supercapacitor

1 Introduction

Redox supercapacitors are an attractive energy storage device that can bridge the gap between a conventional battery and dielectric capacitor due to a combination of high power, fairly high energy density, and long cycle life. It can thus be used as a power source for a variety of potential applications from cellular phones to hybrid electric vehicles. Conducting polymers such as polyaniline (PANI) are promising electrode materials of the redox supercapacitors [1–5], typically demonstrating higher capacitance than electric double-layer capacitor due to high conductivity and good processability. PANI as an electrode material for supercapacitors but has poor cycle life, a critical problem that may originate from gradual degradation during charge/discharge process, during which the charged/uncharged polymeric species can be susceptible to nucleophilic attack by an electrolyte and/or solvent components [6, 7]. The repeated volume change of the PANI electrode during charge/discharge (or doping/undoping) also causes the accumulation of mechanical stress in the PANI matrix that can be directly related to the poor cycle life [8, 9].

In order to improve the cycle performance of a PANI electrode, Nafion was adopted as a positive charge stabilizer to suppress the nucleophilic attack of other species on the PANI matrix during the charging process [7]. Additionally, single- and multi-walled carbon nanotubes (CNT)

J. M. Ko (✉)
Department of Applied Chemistry & Biotechnology, Hanbat National University, Yusong, Daejeon 305-719, South Korea
e-mail: jmko@hanbat.ac.kr

K. S. Ryu
Department of Chemistry, Ulsan University, Ulsan 680-749, South Korea

S. Kim
College of Bionanotechnology, Kyungwon University, Seongnam, Gyeonggi 461-701, South Korea

K. M. Kim (✉)
Research Team of Next-Generation Energy Technology, Electronics and Telecommunications Research Institute (ETRI), Yusong, Daejeon 305-700, South Korea
e-mail: kwang@etri.re.kr

were employed to overcome the mechanical stress-induced degradation of PANI for supercapacitor electrode [8–10]. The excellent mechanical strength and good resiliency of CNT alleviated the mechanical stress in PANI, and thereby the cycle performance could be considerably improved. Alternatively, ruthenium oxide (RuO_2) used as an electrode material of redox supercapacitors is known to show excellent cycle performance and high specific capacitance ($\sim$720 F g^{-1}) [11–14]. Due to the inherently dense morphology of the RuO_2, however, only a very thin surface layer of this material participated in the charge storage process, and the underlying bulk material remained as dead volume, resulting in a reduction in specific capacitance. Many attempts to overcome these drawbacks have been made by synthesizing composites of RuO_2 with activated carbon [15–17], CNTs [18–21], carbon nanofibers [22], and some conducting polymers [23, 24]. For instance, RuO_2/90% activated carbon and RuO_2/CNT composites recently achieved very high capacitance values over 1,000 F g^{-1} [15, 19, 20].

In this study, a PANI and PANI/CNT composite was synthesized, and the effect of CNT on improving the cycleability of supercapacitors was examined. This PANI/CNT composite was then employed as a matrix material to prepare a PANI/CNT/RuO_2 composite in which a small quantity of hydrous RuO_2 was electrodeposited on the PANI/CNT matrix surface to produce a thin layer of hydrous RuO_2. After the evaluation of supercapacitive properties of the PANI, PANI/CNT, and PANI/CNT/RuO_2 electrodes by cyclic voltammetry and other characterization tools, the advantages of each electrode in terms of specific capacitance and cycleability are examined and discussed. In addition, the PANI/CNT/RuO_2 composite electrode is particularly considered as a tool for increasing the utilization of supercapacitive active material.

2 Experimental

CNTs (multi-walled, 20 nm diameter, 5 μm length, purity >90%; Carbon Nano-materials Tech., Pohang, Korea) prepared by chemical vapor deposition was used without further purification. All other chemicals were purchased from Aldrich. The preparation procedures of PANI and PANI/CNT active materials is described elsewhere [25]; 0.856 g of CNT was used. The masses of PANI in the PANI and PANI/CNT active materials were 4.3 and 3.424 g, respectively. To fabricate PANI and PANI/CNT electrodes, slurries were prepared by mixing the PANI or PANI/CNT active material (90 wt.%) with poly(vinylidene fluoride-*co*-hexafluoropropylene) binder (10 wt.%) dissolved in *N*-methyl-2-pyrrolidone. Prior to mixing the binder solution with the electrode active material, dry powders were ball-milled for 12 h at 100 rpm to give a well-dispersed state. For PANI/CNT material, no solid-state reaction between the polymer and CNT occurred during this long-time ball-milling process because the amount of polymer binder applied was as small as 10 wt.%. After adding the binder solution, the milling continued for 24 h at 100 rpm to obtain homogeneous slurries with good dispersion. The slurries were then cast onto one side of Pt foil (1 cm^2) electrode. The other side of Pt foil was sealed with polyimide tape to prevent the transport of electrons and/or carriers on this side. The electrodes were dried overnight in ambient atmosphere and further dried under vacuum at 40 °C for 24 h. To prepare the PANI/CNT/RuO_2 composite electrode, the PANI/CNT-coated electrode was used as a working electrode and the hydrous RuO_2 was galvanostatically deposited on the surface of PANI/CNT by applying a reductive current (5.0 mA cm^{-2}) for 180 s. The 50 °C plating bath contained 5.0 mM of $RuCl_3$ xH_2O, 0.01 M HCl, and 0.1 M KCl (pH 2.0).

Cyclic voltammetry and complex impedance measurements of the PANI-based composite electrodes were performed in a single-compartment cell using an E.G&G (Model 273A) potentiostat/galvanostat with Ag/AgCl (saturated KCl, 0.222 V vs. SHE) as a reference electrode and Pt foil (2 cm × 2 cm) as a counter-electrode. A Luggin capillary was used, in which the tip was 1 or 2 mm from the working electrode to minimize errors from *iR* drop in the electrolyte. For the electrochemical characterizations, a test solution of 1.0 M H_2SO_4 was used as electrolyte because it is commonly employed for evaluating the performance of RuO_2 electrodes, despite the PANI being prepared with 1.0 M $HClO_4$. Prior to use, the electrolyte solution was purged with pure nitrogen for 1 h to remove dissolved oxygen. In the long-term cycle performance test, the solution was covered with a nitrogen blanket. The loading of composite materials on the Pt foil was determined with a digital balance (Metler Toledo) that had a sensitivity of 10.0 μg. The surface morphology of the PANI-based composites was examined using a field-emission scanning electron microscope (XL30SFEG, Philips).

3 Results and discussion

The ratio of PANI in the PANI/CNT composite was 80 wt.%. The ratio of RuO_2 in the PANI/CNT/RuO_2 ternary composite after electrodeposition was estimated to be 7 wt.% metallic Ru by comparing weights before and after deposition. Due to the constant reductive current applied for deposition of RuO_2 it is believed that only metallic Ru is deposited during the initial stage; this is transformed (oxidised) into the amorphous hydrous oxide form (RuO_2)

upon cycling. Surface morphologies of PANI and PANI/CNT composite electrodes (see Fig. 1) were similar to those in an earlier report [25] in which the morphology of pristine CNT was also shown. The granular structure of PANI doped with chloride anions was observed; this was typical to that prepared with perchloric acid [26]. For the PANI/CNT composite, the PANI was uniformly coated on the CNT surface. The diameter of the PANI-coated CNT was ~80 nm, which is a desirable morphology for supercapacitor electrode materials as the high specific surface area can store more double-layer charge to obtain high specific capacitance. The open surface may provide rapid access of the electrolyte into the bulk-phase of the electrode material. The dispersion of Ru species on the PANI/CNT matrix may be confirmed by a precise technique like depth profile analysis of Auger electron spectroscopy [27], but a simple morphological observation was performed in this study. After deposition of RuO_2, the PANI/CNT morphology changed; small globular RuO_2 particles with a diameter of approximately 70–100 nm were distributed on the surface of the PANI/CNT matrix (see Fig. 1c). Effective dispersion of a thin surface layer of hydrous RuO_2 (7 wt.% metallic Ru in the PANI/CNT/RuO_2 electrode) was helpful in utilizing the RuO_2 layer to provide high charge storage and long cycle life.

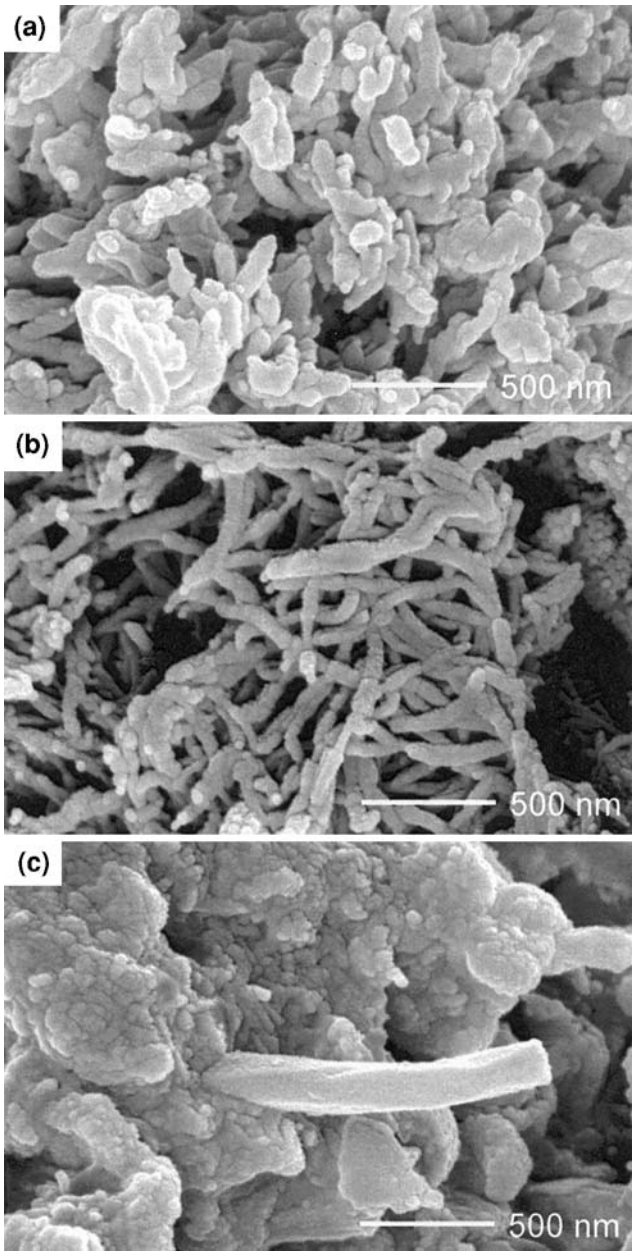

Fig. 1 Scanning electron micrographs of **a** PANI, **b** PANI/CNT, and **c** PANI/CNT/RuO_2 composite electrode materials

As shown in Fig. 2, the electrochemical characteristics of three types of electrode were investigated by cyclic voltammetry at scan rates ranging from 100 to 1,000 mV s^{-1}. The current values in the figures are normalized to the weight of active material (mass of binder are not considered as active material) in the electrodes. PANI-based electrodes are usually known to show bulk faradaic redox behavior at potentials over 0.2 V [28]. All electrodes in this study show the same phenomena; the redox peak position shifts with increase in scan rate to yield a wider potential range between the cathodic and anodic peaks, indicating a capacitance decrease (or revealing the irreversibility) as the *iR* drop becomes significant. Cyclic voltammograms (CVs) of the PANI electrode show a well-defined redox behavior, which agrees with previous work [1, 7]. The distortion in the shape of the CV may be attributed to the limitation of proton diffusion-migration and the *iR* drop in the bulk PANI electrode [1]. As shown in Fig. 2a the cathodic peaks in the range 0.2–0.5 V and their corresponding anodic peaks in the −0.1 to 0.1 V region are attributable to the redox transition of PANI in its oxidation states, that is, between the leucoemeraldine and the emeraldine forms [29, 30]. However, the pair of redox peaks with higher oxidation states of PANI at potentials >0.6 V [27] cannot be clearly shown, due to the degradation of PANI by the attack of water molecules [31].

The CVs of the PANI/CNT and PANI/CNT/RuO_2 electrodes clearly indicate both a redox process at low potential and a double-layer capacitive behavior in the high potential range, in contrast to the behavior of the PANI electrode. The CV shape of the PANI/CNT electrode, compared to the PANI electrode, appears as a partial rectangle at higher potential >0.6 V. That is, the CNT in the PANI/CNT electrode provides a high surface area in the composite, resulting in the development of capacitive properties between 0.6 and 0.8 V. Based on the potential 0.6 V which may be considered as an edge of the partial rectangular CV shape, the anodic current density increases linearly with increase in scan rate. This implies very fast faradaic reactions of capacitive behavior, revealing the

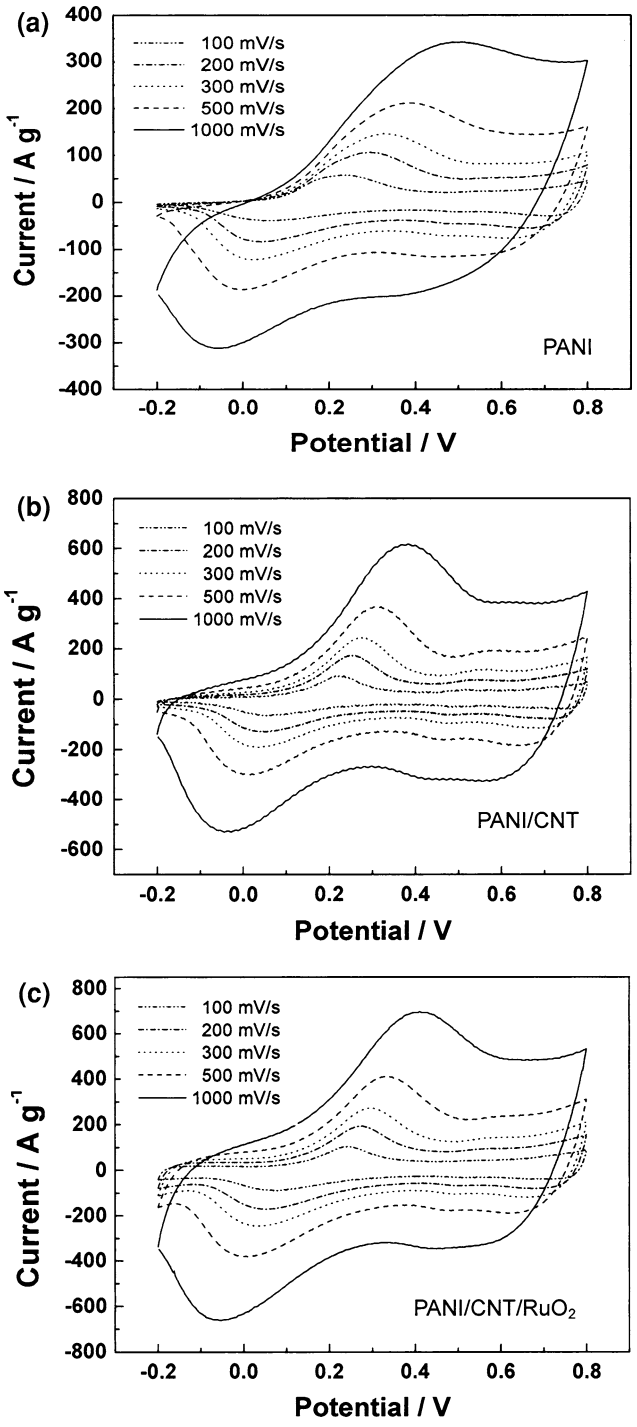

Fig. 2 Cyclic voltammograms of **a** PANI, **b** PANI/CNT, and **c** PANI/CNT/RuO_2 electrodes recorded in 1.0 M H_2SO_4 at various scan rates

high power properties of PANI/CNT and PANI/CNT/RuO_2 composite electrodes [19].

The PANI/CNT/RuO_2 electrode showed no new peaks, compared to pure RuO_2 [22] and CNT/RuO_2 [18, 21], although some increases in current was observed. It is widely accepted that in RuO_2 double injection/expulsion of electrons and protons occurs, whereas in PANI counterion diffusion (anion doping/dedoping) occurs, although protons may inject/expel in the more positive potential range. Considering the charge storage process in PANI and pure RuO_2 electrodes in the aspect of the concomitant exchange of protons and electrons, the PANI and RuO_2 in the PANI/CNT/RuO_2 composite electrode may show synergistic effects during the charge storage process. Also, it seems that effective dispersion of a thin surface layer of hydrous RuO_2 (7 wt.% metallic Ru in the PANI/CNT/RuO_2 electrode) provides high electrochemical utilization in the PANI/CNT/RuO_2 due to the large interfacial area between RuO_2 and CNT. In addition, the PANI/CNT and PANI/CNT/RuO_2 electrodes demonstrate no significant change in the CV shapes, even at the high scan rate of 1,000 mV s^{-1}. Therefore, *iR* loss was no longer considered in the composite electrodes, revealing the high-power characteristics.

The specific capacitance estimated from the CVs is represented as a function of scan rate in Fig. 3. The specific capacitances at 100 mV s^{-1} were 237, 333, and 441 F g^{-1} for PANI, PANI/CNT, and PANI/CNT/RuO_2 composite electrodes, respectively. The capacitance of 333 F g^{-1} for PANI/CNT is slightly lower than the values (350–380 F g^{-1}) for some polymer/CNT electrodes [32, 33]. From a control experiment, the specific capacitance of pure CNT was estimated to be 40 F g^{-1}. By subtracting the double-layer contribution of CNT, it was observed that the PANI/CNT composite electrode delivered an additional capacitance of 56 F g^{-1} (i.e., $333 - 237 - 40 = 56$), which can be understood as a synergistic capacitance. A composite of PANI with CNT can be made by increasing the specific surface area of the PANI, resulting in the enhanced double-layer capacitance of PANI. Alternatively, a thin coating of PANI on CNT can facilitate an effective

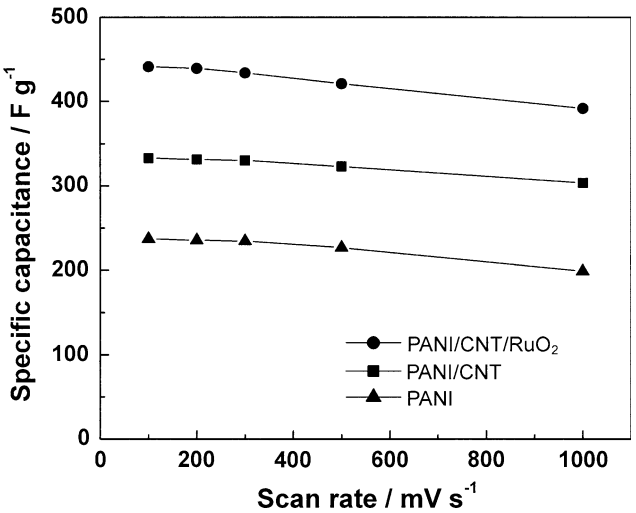

Fig. 3 Specific capacitance of three types of electrodes as a function of scan rate recorded in 1.0 M H_2SO_4

penetration of electrolyte into the volume of PANI, leading to enhanced participation of active material in the charge storage process. The open morphology of the PANI/CNT composite and good electrical conductivity offered by CNT may be considered to play a favorable role in the higher specific capacitance of the PANI/CNT composite electrode.

It was interesting to observe that the PANI/CNT/RuO_2 composite electrode showed higher specific capacitance than that of the PANI/CNT electrode, even for small loadings of RuO_2 (7 wt.% metallic Ru) in the composite. The difference in specific capacitance may originate from a Faradaic pseudo-capacitance of the RuO_2 material. Since the pseudo-capacitance of RuO_2 originates from surface reactions and is proportional to the specific surface area, the PANI/CNT composite appears to be appropriate as a matrix material for the effective surface dispersion of RuO_2, thereby maximizing the specific surface area of RuO_2. The specific capacitance (441 F g^{-1}) of the PANI/CNT/RuO_2 composite at 100 mV s^{-1}, which was based on the combined mass of PANI and RuO_2, was also greater than the values obtained from other composites of RuO_2 with carbonaceous materials [16, 18]. At a scan rate of 1,000 mV s^{-1}, the capacitance retentions were 84, 91, and 89% for the PANI, PANI/CNT, and PANI/CNT/RuO_2 composite electrodes, respectively, when compared with those at 100 mV s^{-1}. The data reflected the high power characteristics of the composite electrodes, which was due to the presence of highly conducting mesoporous CNT in the composite that offers higher electrical conductivity to the active material, and enables the rapid influx of electrolyte into the entire volume of electrode.

The cycle performances of three types of electrodes were investigated to confirm the improvement in cycle life by adopting CNT and/or RuO_2, compared to the PANI electrode. These cyclic stability tests were conducted in the potential range −0.2 to 0.6 V, not from −0.2 to 0.8 V, because we avoided the degradation range (0.6–0.8 V) of PANI by attack of water molecules [31]. Continuous cycling for 10^4 times was performed with CV measurement in 1.0 M H_2SO_4 electrolyte between −0.2 and 0.6 V at a scan rate of 200 mV s^{-1} (see Fig. 4). Each electrode maintains a similar CV shape after 10^4 cycles, except for the decrease in current. Among the three electrodes, however, PANI/CNT/RuO_2 showed distinctive redox peaks, especially, the capacitive currents at both ends of the potential window. This is particularly due to the pseudo-capacitive reactions of RuO_2 in the composite electrode. The specific capacitance estimated from the CVs at 200 mV s^{-1} is shown in Fig. 5. After 10^4 cycles, the capacitance retentions were 51, 66, and 61% for PANI, PANI/CNT, and PANI/CNT/RuO_2 electrodes, respectively, compared to the first cycle. Although the reversibility of all

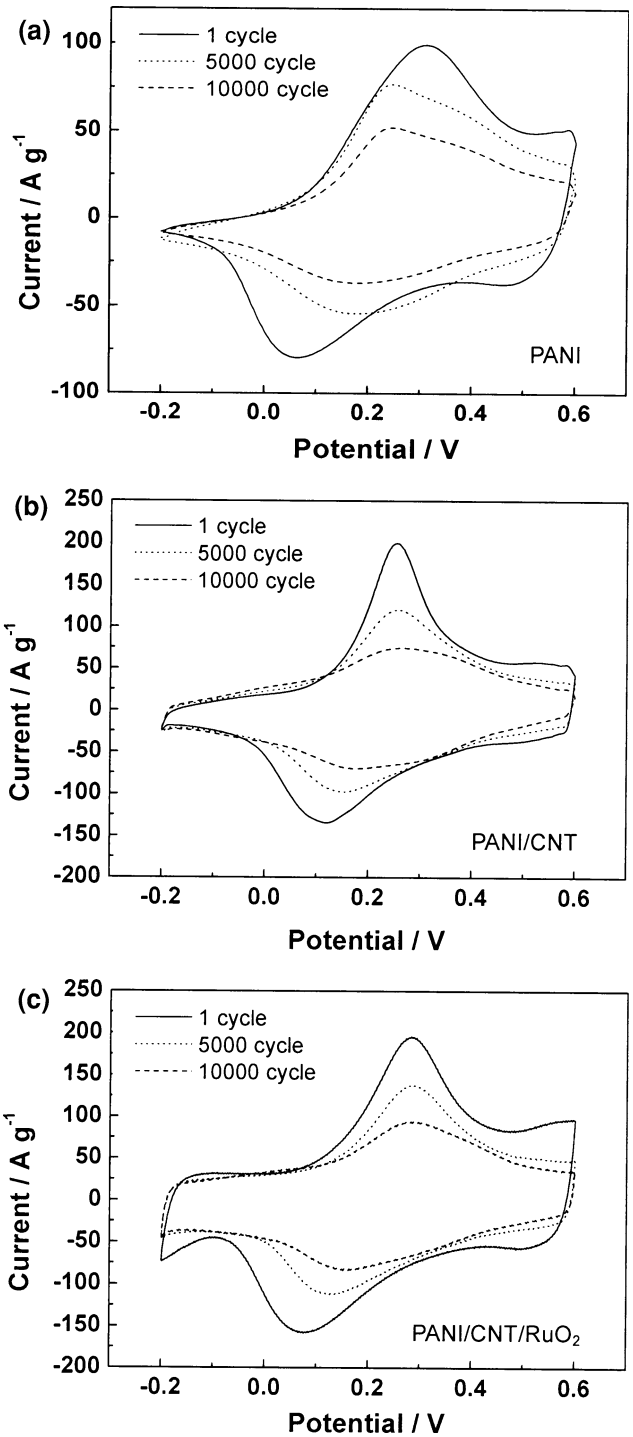

Fig. 4 Cyclic voltammograms of **a** PANI, **b** PANI/CNT, and **c** PANI/CNT/RuO_2 electrodes recorded at a scan rate of 200 mV s^{-1}during cycle performance test in 1.0 M H_2SO_4

electrodes is somewhat poor because of the comparatively higher scan rate (200 mV s^{-1}), the CNT appeared to improve the cycleability of PANI by alleviating the mechanical stress from volume change during the doping/dedoping process. However, the PANI in the PANI/CNT

also underwent mechanical degradation. By a rough quantitative calculation, the improvement in cyclability of PANI due to the CNT was 130% (=66/51 for PANI/CNT vs. PANI at 200 mV s^{-1}) after 10^4 cycles. Compared to the previous result of using Nafion [7] instead of CNT, the improvement in cyclability of PANI was 135% (84/62 for PANI/Nafion vs. PANI at 500 mV s^{-1}) after 10^4 cycles. It is remarkable that CNT and Nafion may offer nearly equal contributions in improving the cycle performance of PANI although slightly different scan rates were applied. On the other hand, the slightly lower capacitance retention of the PANI/CNT/RuO_2 electrode (61%) after 10^4 cycles, compared to the PANI/CNT electrode (66%), is presumed to be due to the dissolution and/or detachment of some RuO_2 from the electrode. However, the order of electrodes with respect to decreasing the loss in specific capacitance is PANI/CNT/RuO_2 (140 F g^{-1}) >PANI/CNT (90 F g^{-1}), indicating that the CNT does not maintain more capacitance in the composites.

Figure 6 shows the complex impedance spectra of the three electrodes, obtained before the cycle performance test and after 10^4 cycles. The PANI/CNT and PANI/CNT/RuO_2 composite electrodes exhibited good capacitor-like behavior with a small diffusion limit. Due to the slight difference in electrode thickness (in the order of $\sim 10^2$ μm excluding the Pt foil) before cycling, a slight difference (~ 0.1 Ω) in the real component of impedance at high frequency was observed. The real component of the impedance spectra at high frequency, corresponding to the solution resistance and electronic/ionic resistance of the electrode film, slightly increased for only the PANI electrode after 10^4 cycles. This indicates that the other electrodes, except for the PANI, exhibited good electrochemical stability over long-term cycling. The impedance spectra of these composite electrodes do not demonstrate notable differences after cycling 10^4 times, although some losses in specific capacitance were observed.

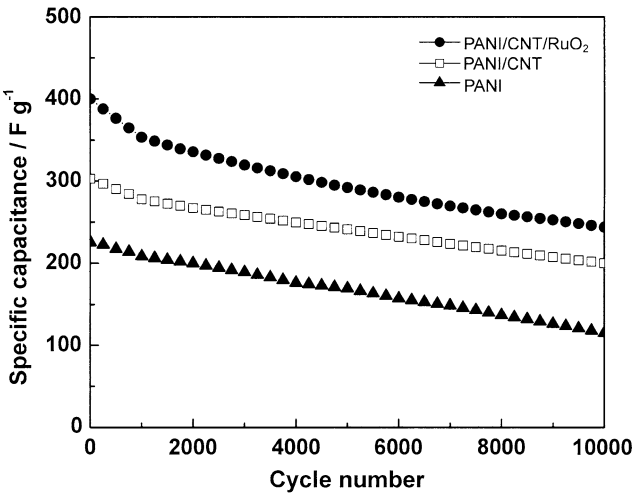

Fig. 5 Specific capacitance of three types of electrodes recorded at a 200 mV s^{-1} as a function of cycle number

4 Conclusions

Electroactive PANI and PANI/CNT were prepared by chemical polymerization. The PANI/CNT composite was used as a matrix for the electrochemical deposition of RuO_2 to produce PANI/CNT/RuO_2. Specific capacitances estimated from cyclic voltammetry were 237, 333, and 441 F g^{-1} (at 100 mV s^{-1}) and 199, 304 and 392 F g^{-1} (at 1,000 mV s^{-1}) for PANI, PANI/CNT and PANI/CNT/RuO_2 composite electrodes, respectively. It seems that the higher specific capacitance of the PANI/CNT composite of PANI was due to the surface area increase and effective

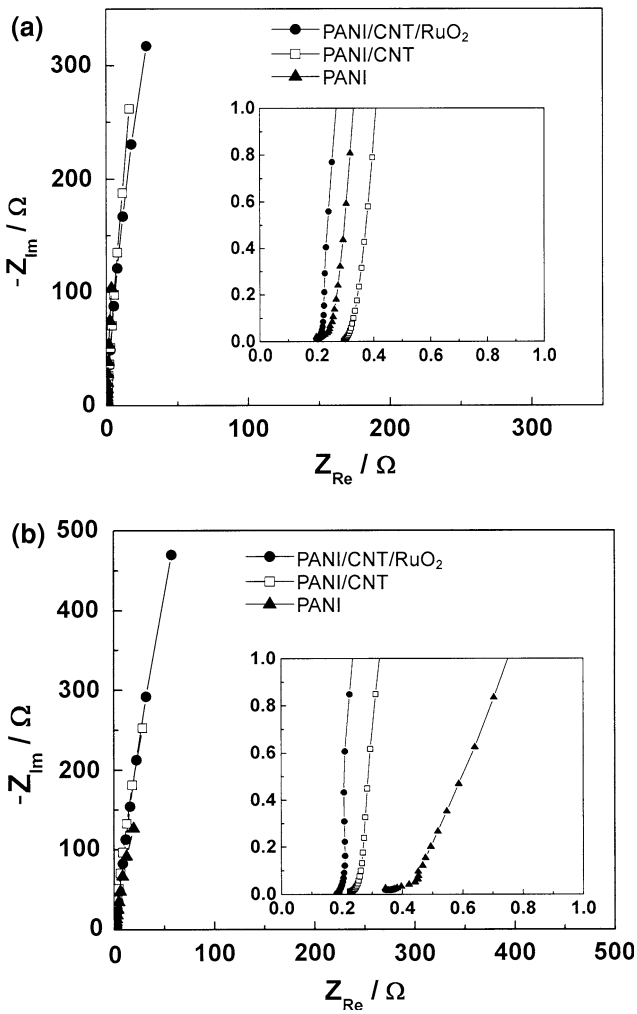

Fig. 6 Nyquist plots of three types of electrodes measured **a** before cycle performance test and **b** after cycling for 10^4 times in the voltage range of −0.2 to 0.6 V at a scan rate of 200 mV s^{-1} (frequency range 10^{-2}–10^4 Hz, d.c. bias 0.5 V vs. Ag/AgCl)

penetration of the electrolyte component into the entire volume of PANI, leading to enhanced participation of active material in the charge storage process. A small loading of RuO_2 (7 wt.% of metallic Ru) in the PANI/CNT/RuO_2 composite improved the capacitance by 108 F g^{-1}, compared to the PANI/CNT electrode. The cycle performance indicated that after 10^4 cycles the capacitance retentions were 51, 66 and 61% for PANI, PANI/CNT, and PANI/CNT/RuO_2 electrodes, respectively. The CNT certainly offers mechanical support to the PANI, thereby enabling the improvement in cycle life. The low capacitance retention of the PANI/CNT/RuO_2 electrode after 10^4 cycles, in comparison with PANI/CNT, was probably due to dissolution and/or detachment of some of the RuO_2 from the electrode.

Acknowledgment One of the authors (JMK) appreciates the financial support for this work through the World-Class University Program (R33-2008-000-10147-0) from the Korean Ministry of Education, Science and Technology.

References

1. Fusalba F, Gouérec P, Villers D, Bélanger D (2001) J Electrochem Soc 148:A1
2. Ryu KS, Kim KM, Park N-G, Park YJ, Chang SH (2002) J Power Sources 103:305
3. Ko JM, Song RY, Yu HJ, Yoon JW, Kim BG, Kim DW (2004) Electrochim Acta 50:873
4. Ryu KS, Jeong SK, Joo J, Kim KM (2007) J Phys Chem B 111:731
5. Ryu KS, Kim KM (2007) J Power Sources 165:420
6. Zhang AQ, Cui CQ, Lee JY (1995) Synth Met 72:217
7. Song RY, Park JH, Sivakkumar SR, Kim SH, Ko JM, Park D-Y, Jo SM, Kim DY (2007) J Power Sources 166:297
8. Khomenko V, Frackowiak D, Béguin F (2005) Electrochim Acta 50:2499
9. Frackowiak E, Khomenko V, Jurewicz K, Lota K, Béguin F (2006) J Power Sources 153:413
10. Gupta V, Miura N (2006) Electrochim Acta 52:1721
11. Zheng JP, Cygan PJ, Jow TR (1995) J Electrochem Soc 142:2699
12. Hu C-C, Huang Y-H (2001) Electrochim Acta 46:3431
13. Hu C-C, Chang K-H, Lin M-C, Wu Y-T (2006) Nano Lett 6:2690
14. Gujar TP, Shinde VR, Lokhande CD, Kim W-Y, Jung K-D, Joo O-S (2007) Electrochem Commun 9:504
15. Hu C-C, Chen W-C (2004) Electrochim Acta 49:3469
16. Dandekar MS, Arabale G, Vijayamohanan K (2005) J Power Sources 141:198
17. Min M, Machida K, Jang JH, Naoi K (2006) J Electrochem Soc 153:A334
18. Arabale G, Wagh D, Kulkarni M, Mulla IS, Vernekar SP, Vijayamohanan K, Rao AM (2003) Chem Phys Lett 376:207
19. Kim I-H, Kim J-H, Kim K-B (2005) Electrochem Solid State Lett 8:A369
20. Kim I-H, Kim J-H, Lee Y-H, Kim K-B (2005) J Electrochem Soc 152:A2170
21. Kim Y-T, Tadai K, Mitani T (2005) J Mater Chem 15:4914
22. Lee BJ, Sivakkumar SR, Ko JM, Kim JH, Jo SM, Kim DY (2007) J Power Sources 168:546
23. Hong J-I, Yeo I-H, Paik W-K (2001) J Electrochem Soc 148:A156
24. Huang L-M, Lin H-Z, Wen T-C, Gopalan A (2006) Electrochim Acta 52:1058
25. Sivakkumar SR, Kim D-W (2007) J Electrochem Soc 154:A134
26. Ryu KS, Wu X, Lee Y-G, Chang SH (2003) J Appl Polym Sci 89:1300
27. Hu C-C, Chen E, Lin J-Y (2002) Electrochim Acta 47:2741
28. Hu C-C, Chu C-H (2001) J Electroanal Chem 503:105
29. Genies EM, Lapkowski M (1987) J Electroanal Chem 220:67
30. Focke WW, Wnek GE, Wei Y (1987) J Phys Chem 91:5813
31. Lin S-M, Wen T-C (1994) Electrochim Acta 39:393
32. Liu T, Sreekumar TV, Kumar S, Hauge RH, Smalley RE (2003) Carbon 41:2440
33. Zhou C, Kumar S, Doyle CD, Tour JM (2005) Chem Mater 17:1997